https://doi.org/10.15407/exp-oncology.2024.02.087

A. BOSTANCI [1, *], O. DOGANLAR [2, *]

[1] Department of Genetics and Bioengineering, Trakya University, Edirne, Turkey
[2] Department of Medical Biology, Faculty of Medicine, Trakya University, Edirne, Turkey

* Correspondence: Email: aytensari@trakya.edu.tr
oguzhandoganlar@trakya.edu.tr

MELATONIN ENHANCES TEMOZOLOMIDE-INDUCED APOPTOSIS IN GLIOBLASTOMA AND NEUROBLASTOMA CELLS

Background. The combination of temozolomide (TMZ) and paclitaxel (PTX) is the most commonly used chemotherapy regimen for glioblastoma, but there is no specific treatment for neuroblastoma due to the acquired multidrug resistance. Approximately half of treated glioblastoma patients develop resistance to TMZ and experience serious side effects. Melatonin (MEL), a multifunctional hormone long known for its antitumor effects, has a great advantage in combination cancer therapy thanks to its ability to affect tumors differently than normal cells. **Aim**. This study aims to evaluate the *in vitro* inhibitory effects of MEL in combination with TMZ on cancer cell viability and to elucidate the underlying mechanisms in the glioblastoma and neuroblastoma cell lines. **Materials and Methods**. C6 (*Rattus norvegicus*) and N1E-115 (*Mus musculus*) cancer cell lines and C8-D1A (mice) healthy cell lines were used. Cell proliferation was evaluated using the MTT test. IC_{50} values were determined by probit analysis. Two concentrations of TMZ (IC_{50} and 1/2 IC_{50}) were used to induce cytotoxicity in the C6 and N1E-115 cell lines, both alone and in combination with PXT and MEL (all at IC_{50}). The viable, dead, and apoptotic cells were determined by image-based cytometry using Annexin V/PI staining. The gene expression related to signaling pathways was assessed by the quantitative reverse transcription polymerase chain reaction (qRT-PCR), and key proteins were identified by the Western blot analysis. **Results**. MTT assay showed that the combination of TMZ and MEL significantly reduces the viability of both glioblastoma and neuroblastoma cells compared to the vehicle-treated controls. Notably, MEL combined with 1/2 IC_{50} TMZ showed a significant death rate of cancer cells compared to controls and PTX. According to qRT-PCR data, the TMZ + MEL combination resulted in the upregulation of the genes of antioxidative enzymes (*Sod1* and *Sod2*) and DNA repair genes (*Mlh1*, *Exo1*, and *Rad18*) in both cell lines. Moreover, the levels of *Nfkb1* and *Pik3cg* were significantly reduced following the TMZ + MEL treatment. The combination of MEL with TMZ also enhanced the cell cycle arrest and increased the expression of p53 and pro-apoptotic proteins (Bax and caspase-3), while significantly decreasing the expression of anti-apoptotic protein Bcl-2. **Conclusions**. Our findings indicate that the combination of MEL with a low dose of TMZ may serve as an upstream inducer of apoptosis. This suggests the potential development of a novel selective therapeutic strategy as an alternative to TMZ for the treatment of both glioblastoma and neuroblastoma.

Keywords: melatonin, glioblastoma, neuroblastoma, temozolomide, cancer treatment.

Citation: Bostanci A, Doganlar O. Melatonin enhances temozolomide-induced apoptosis in glioblastoma and neuroblastoma cells . *Exp Oncol.* 2024; 46(2): 87-100. https://doi.org/10.15407/exp-oncology.2024.02.087

Glioblastoma multiforme (GBM, grade IV glioma by WHO) is the most aggressive type of malignant glioma in adults. In the standard treatment regimen, surgical resection is performed first when the location and size of the tumor are appropriate [1—3]. Standard treatment of GBM involves the initial maximal surgical resection followed by concurrent chemoradiotherapy and adjuvant temozolomide (TMZ) to avoid recurrence and prolong median survival [4]. TMZ is a second-generation alkylating agent used in the treatment of GBM. It promotes cell apoptosis while causing DNA strand breaks during cell replication [5]. Although survival progresses positively with chemotherapy for approximately the first 2.5 months [2], current therapeutic treatment is a rigid schedule. This method only slows down the rate of tumor progression [6], and the average survival time is limited to approximately 14.6 months [7]. The most notable obstacles in traditional treatments are the inability to achieve adequate drug absorption in the brain due to the protective blood-brain barrier and the inherent resistance of GBM cells to the induction of cell death [6, 8]. In addition, the presence of glioblastoma stem cells in a hypoxic tumor environment, phenotypic and genotypic heterogeneity, and abnormal signaling pathways increase the need for the administration of high doses of chemotherapeutic drugs, which worsens their side effects [9]. Despite advances in multimodal treatment, including high-dose chemotherapy, radiation therapy, and stem cell transplantation, the 5-year survival rate in patients with a high-risk disease is less than 50%, suggesting that new treatment strategies need to be investigated [10]. For this reason, therapy alternatives and adjuvant treatments with natural substances have recently begun to be investigated [7].

Neuroblastoma (NB) is a pediatric tumor that originates from the developing sympathetic nervous system and is responsible for 15% of childhood cancer mortality [11, 12]. Treatment protocols for NB are determined according to "risk group" criteria [10]. The current clinical strategy of high-risk NB includes multimodal chemotherapy, surgical resection, radiotherapy, and immunotherapy options. NB has a heterogeneous disease presentation that can regress spontaneously or lead to fatal outcomes. Although high-risk NB initially appears to respond to intensive chemotherapy, relapses frequently occur, with fatal outcomes occurring in approximately 50% of the cases [13]. This highlights the need for a better understanding of disseminated NB and its therapeutic vulnerabilities [11]. Children who fail first-line treatment are unlikely to improve with subsequent treatments and have a dismal prognosis, with survival rates of approximately 5% to 10% [14].

Paclitaxel (PTX) is a powerful anticancer drug originating from plants. It acts by providing microtubule stabilization during cell division, leading to mitotic arrest and subsequent cell death [15]. Combinatorial administration of TMZ and PTX causes high cytotoxicity and apoptosis in glioblastoma cells [16]. It is important to note that PTX, unlike TMZ, does not cross the blood-brain barrier [17].

Melatonin (MEL, N-acetyl-5-methoxytryptamine) is an endogenous neurohormone secreted mainly from the pineal gland [18, 19]. MEL suppresses tumor growth and development by inducing apoptosis in cancerous cells. It regulates immune system responses and works as an anticancer agent. In addition, it has been proven by recent studies that it protects healthy cells, reducing their potential to develop neoplasms [20]. It has also been reported to increase sensitivity to chemotherapeutic agents in resistant types of some cancers [21, 22]. When combined with anti-cancer drugs, MEL increases the potency of chemotherapeutic treatments [23]. It inhibits multiple pathways that ensure survival in tumor cells [24]. We reasoned that combinatorial treatment with MEL and TMZ may offer the potential for GBM chemotherapy. Therefore, successfully combating drug resistance, bypassing the blood-brain barrier, and delivering an effective chemotherapy combination may only be possible with the development of more powerful strategies [25]. In our study, we aimed to show that MEL is a natural potential therapeutic agent by using it alone or in combination to improve conventional treatments and reduce the unwanted side effects of chemotherapy on healthy cells [26]. We investigated the effects of the TMZ + MEL and TMZ + PTX combinations on cell growth and apoptosis in C6 rat glioma cells, N1E-115 mouse NB cells, and C8-D1A mouse astrocytic cells. Additionally, we evaluated whether the combination of MEL with TMZ produces a cytotoxic effect in glioma cells and analyzed the relevant cell death mechanisms.

Materials and Methods

Chemicals. Dulbecco's Modified Eagle Medium (DMEM (319-020-CL), HAM'S F-12 (Ham's F-12 Nutrient Mixture, 318-010-CL), 0.05% Trypsin-EDTA (352-542-EL), and penicillin/streptomycin (Gibco) were purchased from Multicell, Wisent Bio Product, Canada. Fetal bovine serum was obtained from Capricorn Scientific, Germany. Ethanol and DMSO were obtained from Merck, Germany. 10X Dulbecco's phosphate-buffered saline, molecular grade water (DNAase/RNAase free water), and power SYBR® Green Master mix were purchased from Thermo Fisher Scientific, USA. Temozolomide was purchased from Santa Cruz Biotechnology, USA. Melatonin and paclitaxel — from Sigma-Aldrich, USA.

Kits. MTT salt solution (3-4,5-dimethylthiazol-2-yl)-2,5-diphenyltetrazolium bromide) (A-3338-56) was obtained from Biomatik, USA. Tali® Apoptosis Kit — Annexin V Alexa Fluor® 488 and propidium iodide, PureLink™ RNA Mini Kit (# 12183018A), High Capacity cDNA Reverse Transcription Kit (# 4368813), NuPAGE™ 4 to 12%, Bis-Tris, 1.0 mm, Mini Protein Gel (# NP0321BOX), 20X Bolt™ MOPS SDS Running Buffer, NuPAGE™ Sample Reducing Agent, 4X Bolt™ LDS Sample Buffer were purchased from Thermo Fisher Scientific, USA. The RIPA Lysis Buffer System (# sc-24948) was obtained from Santa Cruz Biotechnology (CA, USA).

Antibodies. The following antibodies were used in the current study: anti-BCL-2 (N-19) rabbit polyclonal antibody (# Sc-492), anti-Bax (B-9) mouse monoclonal antibody (# Sc-7480), anti-caspase-3 (4.1.18) mouse monoclonal antibody (# Sc-65497), anti-NFκB p65 (A) rabbit polyclonal antibody (# Sc-109), and anti-p-IκB-α (B-9) mouse monoclonal antibody (# Sc-8404). All these antibodies were purchased from Santa Cruz Biotechnology, USA. Anti-PI3K p85-α (6G10) mouse monoclonal antibody (# NBP2-22212) and anti-beta-actin (NB600-503) was obtained from Novus Biologicals, USA.

Cell lines and culture conditions. Rat glioma cell line C6 (ATCC® CCL-107™), mouse NB cell line N1E-115 (ATCC® CRL-2263™), and mouse astrocyte type I cell line C8-D1A (ATCC® CRL-2541™) were purchased from the American Type Culture Collection (ATCC). Cells were cultured in a nutrient mixture containing equal proportions of DMEM and F-12 medium supplemented with 10% fetal bovine serum, 100 U/ml penicillin/streptomycin in an incubator at 37 °C and 5% CO_2.

Treatment groups. (1) Control group (n = 4) — cells were cultured in a medium containing DMSO at a final concentration of 0.1%;

(2) TMZ group (n = 4) — cells were treated with TMZ alone (62.5—2000 μM);

(3) TMZ + MEL group (n = 4) — cells were treated with TMZ (62.5—2000 μM) and MEL (125—4000 μM);

(4) TMZ + PTX group (n = 4) — cells were treated with TMZ (62.5—2000 μM) and PTX (0.78—25 nM). TMZ, MEL, and PTX were dissolved in 0.1% DMSO.

MTT assay. C6, N1E-115, and C8-D1A cells were seeded in 96-well plates at a density of 3×10^3 cells/well and incubated for 72 h at 37 °C. The cells were then treated with TMZ, TMZ + MEL, TMZ + PTX, or vehicle (final concentration 0.1% DMSO). Doses containing eight different dilution concentrations of TMZ and six different dilution concentrations of MEL and PTX were serially prepared with DNase/RNase-free water, added to the growth medium, and cultured. A 20 μl of MTT (5 μg/ml) solution was applied to each well of the drug-treated plate. After 2—4 h of incubation, the medium containing MTT was removed. Then, 200 μl of ultrapure DMSO was added to each well, and the enzymatic dye was allowed to dissolve homogeneously (30—60 min). After incubation, the absorbance values were measured at a wavelength of 492 nm using a spectrophotometer (Thermo Scientific™ Multiskan™ USA). The absorbance values were calculated as the percent vitality. IC_{50} values were determined by a probit analysis.

Annexin V/propidium iodide staining. To evaluate the apoptotic effects of therapeutic agents, cells were seeded in 25 cm^2 flasks in 3 replications. Combinations of 1/2 IC_{50} TMZ with PTX or MEL IC_{50} at a ratio of 1 : 1 were added to each cell line. After 72 h, cells were harvested and analyzed with the Tali® Image-Based Cytometer (Life Technologies, USA).

RNA isolation, reverse transcription, and qRT-PCR assay. Total RNA isolation of cells was performed using an RNA PureLink® RNA Mini Kit (Life Sciences, USA) following the manufacturer's instructions. cDNAs were amplified using a High Capacity cDNA Reverse Transcription Kit accor-

ding to the manufacturer's protocol (ThermoFisher Scientific, USA). To assess the gene expression levels, the quantitative real-time PCR (qRT-PCR) was performed using the Applied Biosystems™ QuantStudio™ 5 Flex Real-Time PCR System, a 384-well system, in accordance with the SYBR Green qPCR Mastermix protocol. The gene expressions were determined by the threshold cycle number (Ct) and normalized to the endogenous control of *β-actin* using the $2^{-\Delta\Delta CT}$ method and proportionally expressed in comparison with the control. The primers used in the qRT-PCR are given in Supplementary Table 1.

Western blot analysis. C6 and N1E-115 cells were seeded at 1×10^6 cells/well in 6-well plates and incubated at 37 °C in a CO_2 incubator for 24 h, followed by the treatment with TMZ, TMZ + MEL, or TMZ + PTX for 72 h. The cells were collected, and protein extraction was performed based on the RIPA Lysis Buffer Kit protocol (Santa Cruz Biotechnology, USA). Determination of the concentration of protein samples was performed by measuring UV absorbance at 280 nm. C6 and N1E-115 cells were extracted, separated by 8%—12% polyacrylamide gel, and then proteins were transferred to the iBlot® Transfer Stack PVDF membrane (Life Technologies , USA). The antibodies were diluted in an antibody binding buffer according to the band intensity and incubated with the indicated antibodies overnight under darkroom conditions (+4 °C). The bound antibodies were detected using the appropriate anti-rabbit or anti-mouse IgG using a chemiluminescence Western blot substrate kit (Thermo Fisher Scientific, USA). The intensity of the bands was visualized and quantified with a gel imaging system (Bio-Rad ChemiDoc MP System, USA).

Statistical analysis. The spectrophotometric results of the MTT assay were determined by a probit analysis. One-way ANOVA analysis was performed to evaluate the difference between the mean of expression values obtained by the ΔΔCt method for live–dead and apoptotic cell values, qRT-PCR and the endogenous control gene β-actin, and the relative fold changes in protein level values were determined by Tukey HSD. The statistical analyses were performed using SPSS 20, University License (IBM, USA) and Graphpad Prism 5 statistical programs. The differences were considered significant when $p \leq 0.05$.

Results

IC_{50} values of TMZ, MEL, and PTX. We first determined the IC_{50} values of TMZ, MEL, and PTX in C6 and N1E-115 cells using the MTT assay. Cells were incubated with a vehicle as a control in addition to TMZ (62.5—2000 μM), MEL (125—4000 μM), and PTX (0.78—25 nM) for 72 h. As shown in Fig. 1, the IC_{50} values of TMZ, MEL, and PTX for C6 cells were 1732.101 μM, 3691.235 μM, and 6.305 nM, respectively. The IC_{50} values of TMZ, MEL, and PTX for N1E-115 cells were 1738.404 μM, 2571.413 μM, and 8.604 nM, respectively (Fig. 1).

A combination of 1/2 IC_{50} dose of TMZ + MEL is more effective in inhibiting cell viability compared to full IC_{50} dose of TMZ + MEL. TMZ and other drugs together were first applied to C6, N1E-115, and C8-D1A cells for 72 h (1 : 1 ratio). In the second set of experiments, half the IC_{50} dose of TMZ was used in combination with the IC_{50} doses of other drugs (1/2 : 1 ratio) inboth cancer and healthy cells for 72 h. The results suggested the lowest cell survival in C6 and N1E-115 cells treated with the 1 : 1 IC_{50} TMZ + MEL combination. When we evaluated the application of 1/2 IC_{50} TMZ in combination with MEL or PTX, a much better inhibitory effect was observed in C6 and N1E-115 cells than the full IC_{50} TMZ ratio (Fig. 2, *a*, *b*). The impact of the combination treatment on the survival of healthy astrocytes (C8-D1A) had the least cytotoxic effect in the 1/2 IC_{50} TMZ + MEL group compared to the other bunches (Fig. 2, *c*). Therefore, a 1/2 IC_{50} dose of TMZ was used in the following experiments.

Determination of apoptotic cell death by Tali cytometry analysis. Our analysis revealed that both 1/2 IC_{50} TMZ + MEL and 1/2 IC_{50} TMZ + PTX induced cell death as evidenced by an increase in the percentage of apoptotic and necrotic cells in C6 and N1E-115 cells. Concomitantly, there was a significant reduction in the percentage of the live cells in the groups treated with 1/2 IC_{50} TMZ + MEL and 1/2 IC_{50} TMZ + PTX compared to the control cells (Fig. 3). Nevertheless, no significant increase in the apoptotic cell percentage in C6 and N1E-115 cells treated with 1/2 IC_{50} TMZ + MEL and 1/2 IC_{50} TMZ + PTX compared to control cells was observed.

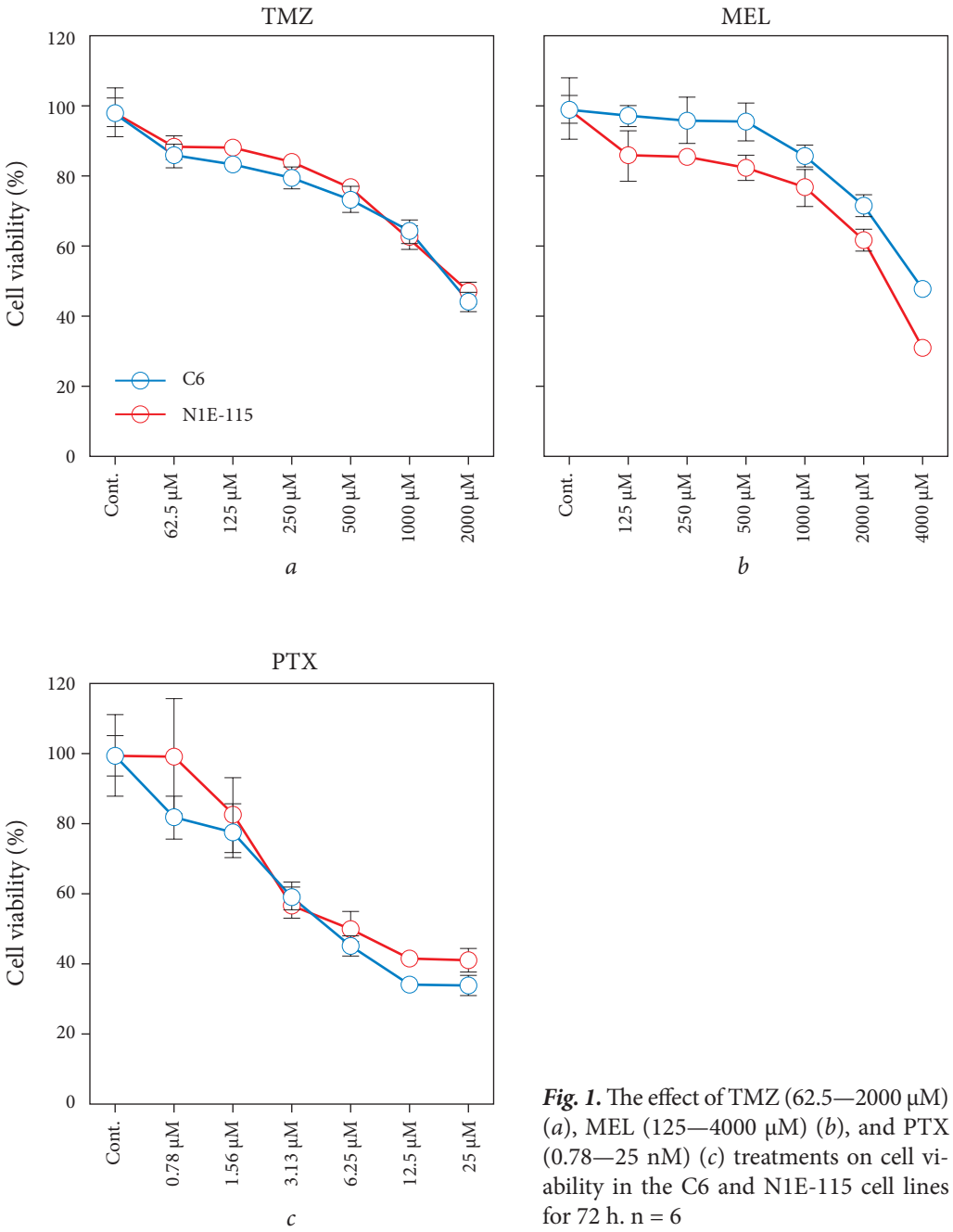

Fig. 1. The effect of TMZ (62.5—2000 μM) (*a*), MEL (125—4000 μM) (*b*), and PTX (0.78—25 nM) (*c*) treatments on cell viability in the C6 and N1E-115 cell lines for 72 h. n = 6

1/2 IC_{50} TMZ + MEL treatment affects multiple signaling pathways in C6 and N1E-115 cell lines. The study explored the effects of combining TMZ and MEL treatments on the C6 and N1E-115 cell lines. The hierarchical clustering analysis of gene expression data revealed the distinct clustering of the TMZ + MEL group compared to the control, TMZ alone, and the TMZ + PTX groups in both cell lines (Fig. 4). Notably, the treatment with 1/2 IC_{50} doses of TMZ + MEL for 72 h led to the upregulation of antioxidative enzymes such as superoxide dismutase (*Sod1*) and superoxide dismutase 2 (*Sod2*), particularly prominent in the C6 cells (Fig. 5).

In the C6 cell line, the TMZ + MEL combination triggered the expression of the tumor suppressor *Tp53*, a major initiator of apoptosis. This activation subsequently led to a comprehensive apoptotic signaling cascade, evidenced by increased expression of the *Bax/Bcl2* gene rate as well as the elevated levels of caspase-3 protein (Fig. 6, *a*, *b*). Additionally, *Casp8* gene expression was significantly upregulated in the TMZ + MEL group compared to the control (Fig. 5). In the N1E-115 cell line, the com-

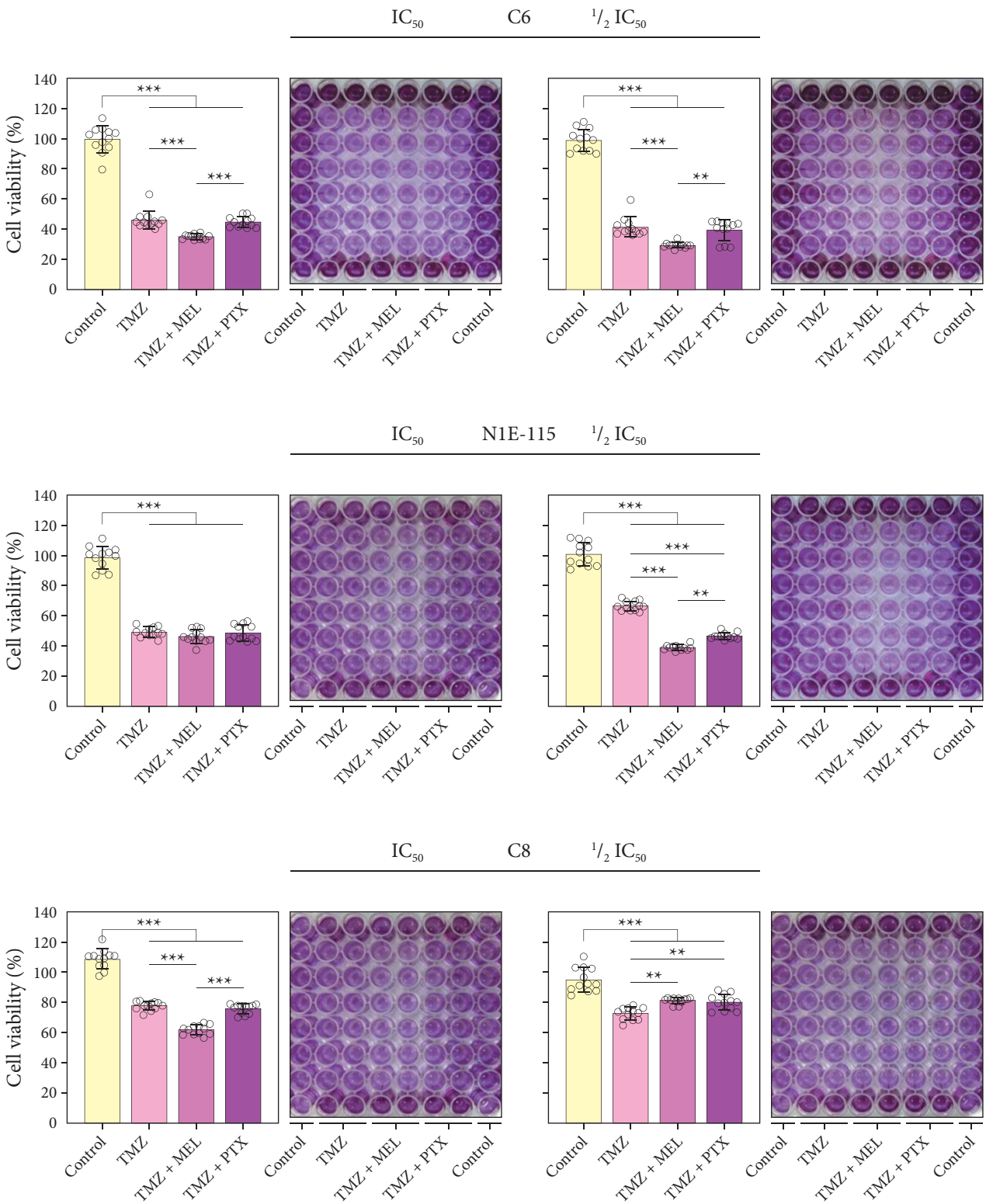

Fig. 2. The effects of the combinations of TMZ IC_{50} or ½ IC_{50} with MEL or PTX on the viability of C6, N1E-115, and C8-D1A cells. % of viable cells was determined by the MTT test. Control — vehicle-treated cells. The doses of TMZ, MEL, and PTX for C8-D1A cells were as for C6 cells. Data were represented as the mean ± SE. One-way ANOVA, Tukey, HSD test, ** $p \leq 0.01$, *** $p \leq 0.001$ (TMZ IC_{50} 1732.101 μM, ½ IC_{50} 866.051 μM, MEL IC_{50} 3691.235 μM, PTX IC_{50} 6.305 nM for C6 cells, TMZ IC_{50} 1738.404 μM, ½ IC_{50} 869.202 μM, MEL IC_{50} 2571.413 μM, PTX IC_{50} 8.604 nM for N1E-115 cells)

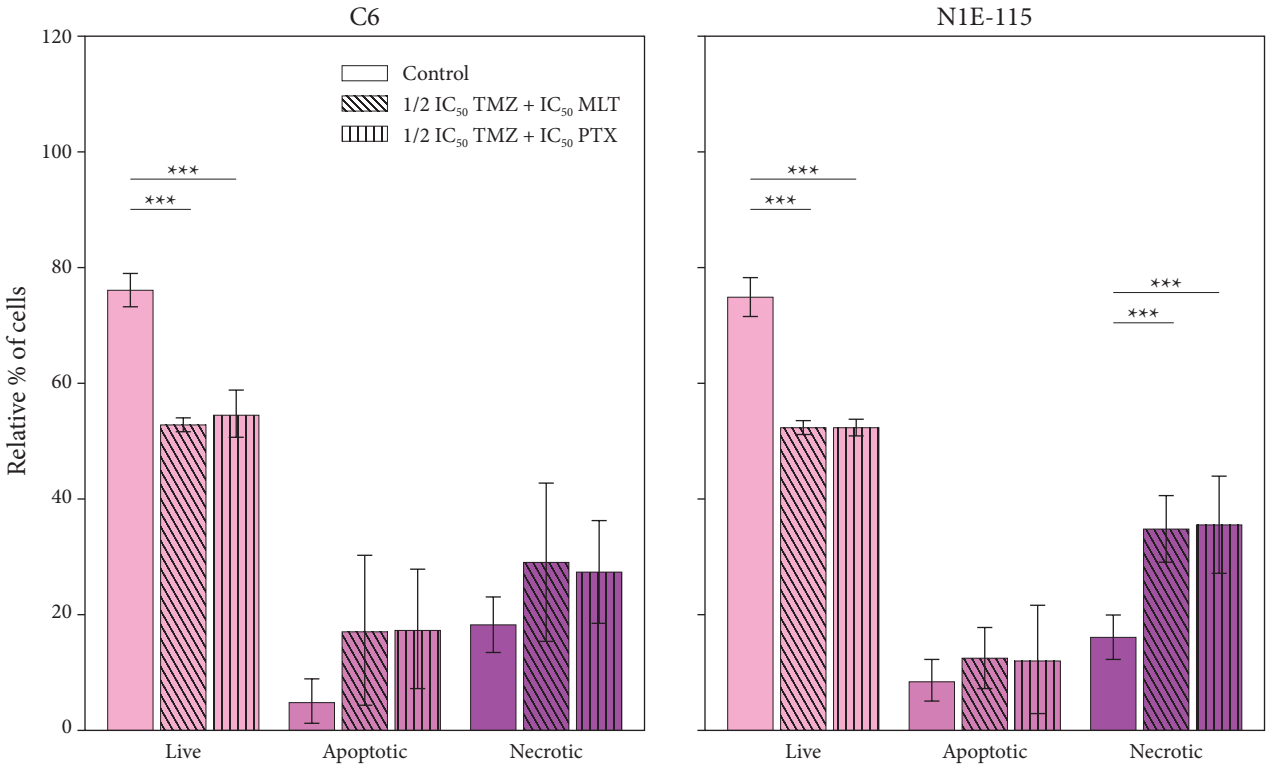

Fig. 3. The percentage of live, apoptotic, and necrotic C6 and N1E-115 cells stained with Annexin V/propidium iodide kit for image-based cytometry. Data are presented as the mean values of percentages for each group ± SE. n = 6. *** indicates significantly different values compared to their respective controls analyzed by a one-way ANOVA, Duncan test ($p \leq 0.001$)

bination treatments exhibited a strong cell arrest and an increase in *Tp53* gene expression levels. Moreover, the protein expression of PI3K p85-α in C6 cells was suppressed proportionally to NF-kB p65 protein levels, especially under the TMZ + MEL treatment (Fig. 6, *d*). Functionally, apoptosis was induced in both cell lines after TMZ + MEL treatment, which was characterized by the engagement of the mitochondrial apoptosis pathway. The *TNF-α/Casp8* axis was also activated by the TMZ + MEL combination, contributing to the apoptotic response observed in the tumor cell lines (Fig. 5). In contrast, the combination treatments with TMZ induced a notably low apoptotic signal in healthy brain astrocytes, with many combination groups showing no significant change in pro-apoptotic gene expression compared to the control. These findings indicate that the combination TMZ + MEL treatment exerts profound effects on multiple signaling pathways. Specifically, it leads to the upregulation of the DNA repair genes such as *Mlh1*, *Exo1*, and Rad18 (Fig. 5), the modulation of antioxidative enzymes, the inhibition of the *Nfkb1* and *Pi3k/Akt1* signaling pathways, and ultimately induces apoptosis through the caspase-mediated mitochondrial pathway (Supplementary Tables 1 and 2). [1]

Discussion

Combinatorial therapies that incorporate natural ingredients along with traditional treatments like chemotherapy have shown promise in enhancing effectiveness and reducing side effects in cancer treatment, particularly for aggressive tumors like GBM and NB [27, 28]. In our study examining combination therapies, we discovered that integrating the natural substance MEL with chemotherapy medications like TMZ yields a beneficial impact on treatment. We have found that using half the IC_{50} concentration of TMZ with MEL results in significant cell death in cancerous cell lines, especially glioblastoma cells. Our studies show that this combination is more potent while causing

[1] You can access supplementary Tables 1 and 2 from this link (Öğr. Gör. Dr. Ayten BOSTANCI | Personel WEB Havuzu | T.C. Trakya Üniversitesi)

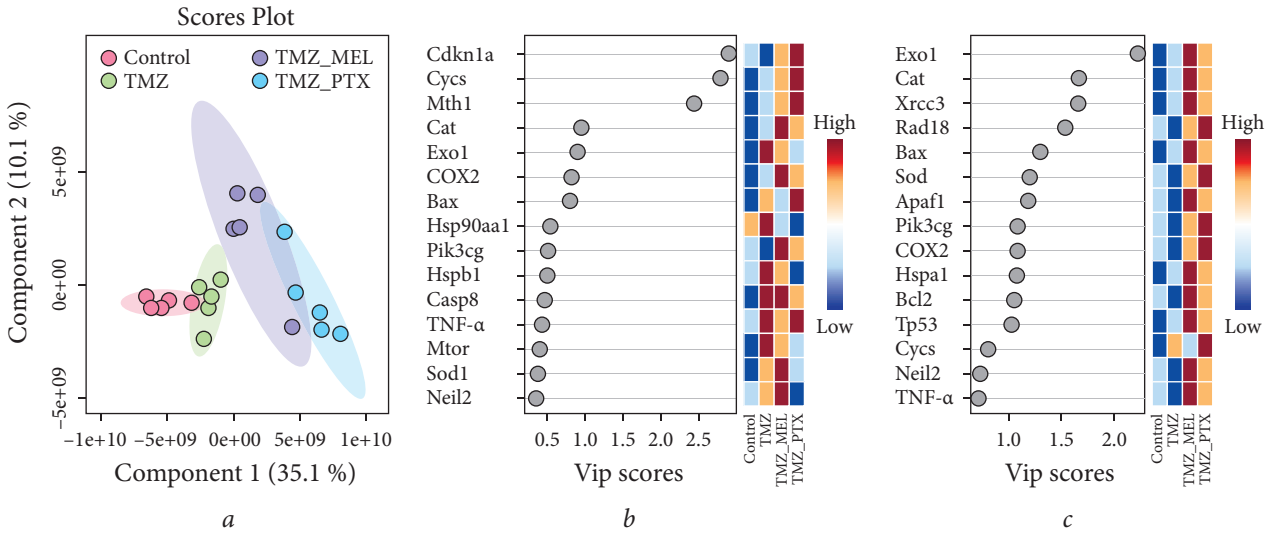
Scores Plot
Control
TMZ
TMZ_MEL
TMZ_PTX
Component 2 (10.1 %)
Component 1 (35.1 %)
Cdkn1a
Cycs
Mth1
Cat
Exo1
COX2
Bax
Hsp90aa1
Pik3cg
Hspb1
Casp8
TNF-α
Mtor
Sod1
Neil2
Vip scores
High
Low
Exo1
Cat
Xrcc3
Rad18
Bax
Sod
Apaf1
Pik3cg
COX2
Hspa1
Bcl2
Tp53
Cycs
Neil2
TNF-α

a *b* *c*

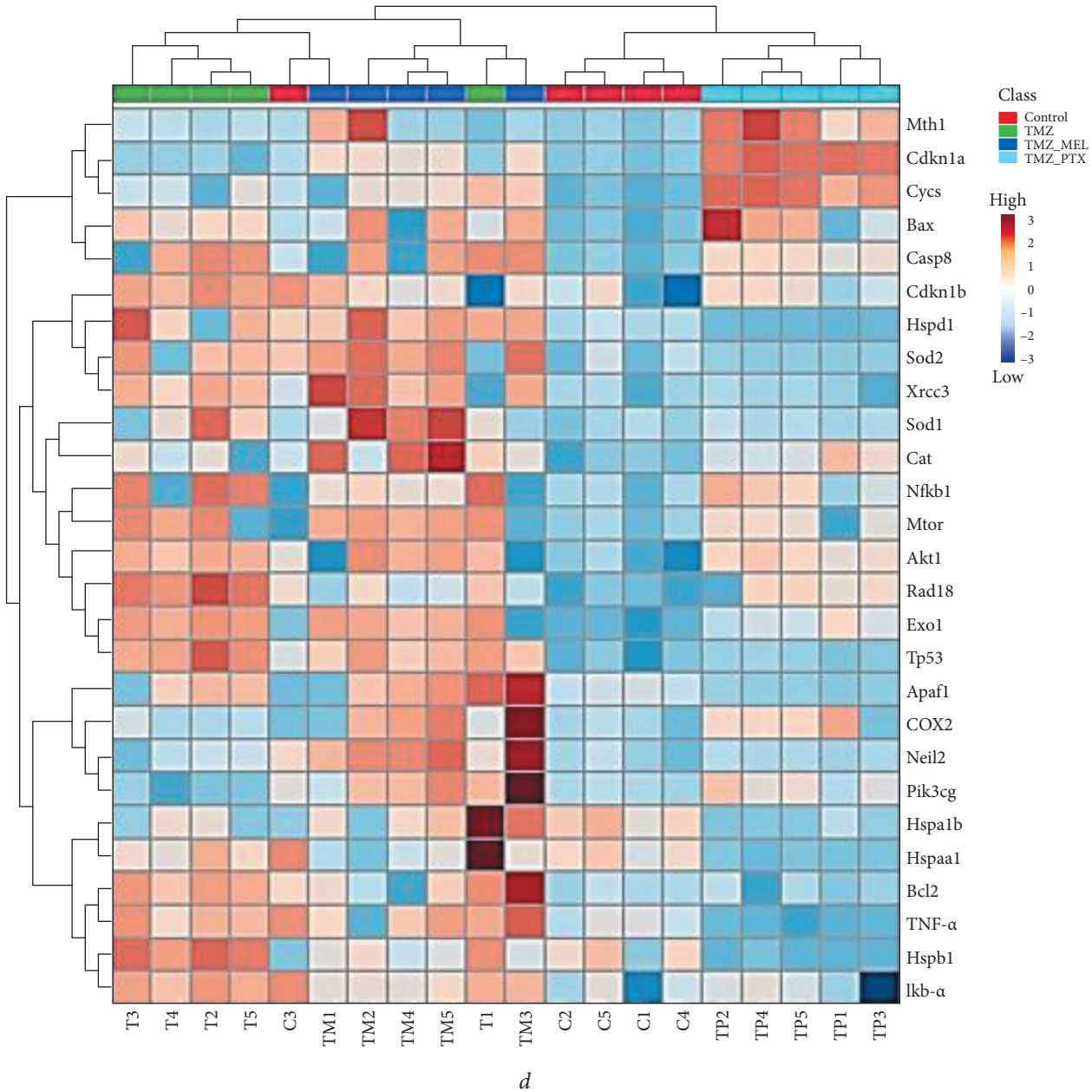
Class
Control
TMZ
TMZ_MEL
TMZ_PTX
High
Low
Mth1
Cdkn1a
Cycs
Bax
Casp8
Cdkn1b
Hspd1
Sod2
Xrcc3
Sod1
Cat
Nfkb1
Mtor
Akt1
Rad18
Exo1
Tp53
Apaf1
COX2
Neil2
Pik3cg
Hspa1b
Hspaa1
Bcl2
TNF-α
Hspb1
Ikb-α
T3 T4 T2 T5 C3 TM1 TM2 TM4 TM5 T1 TM3 C2 C5 C1 C4 TP2 TP4 TP5 TP1 TP3

d

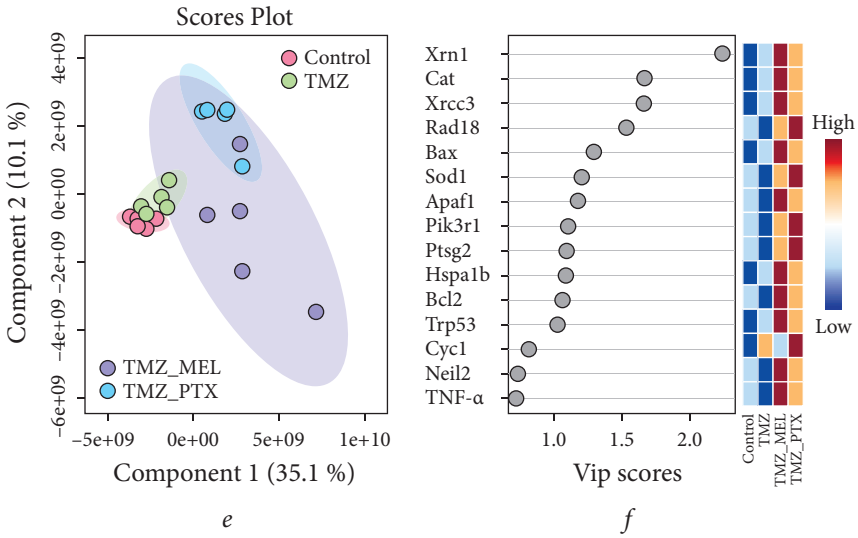

e *f*

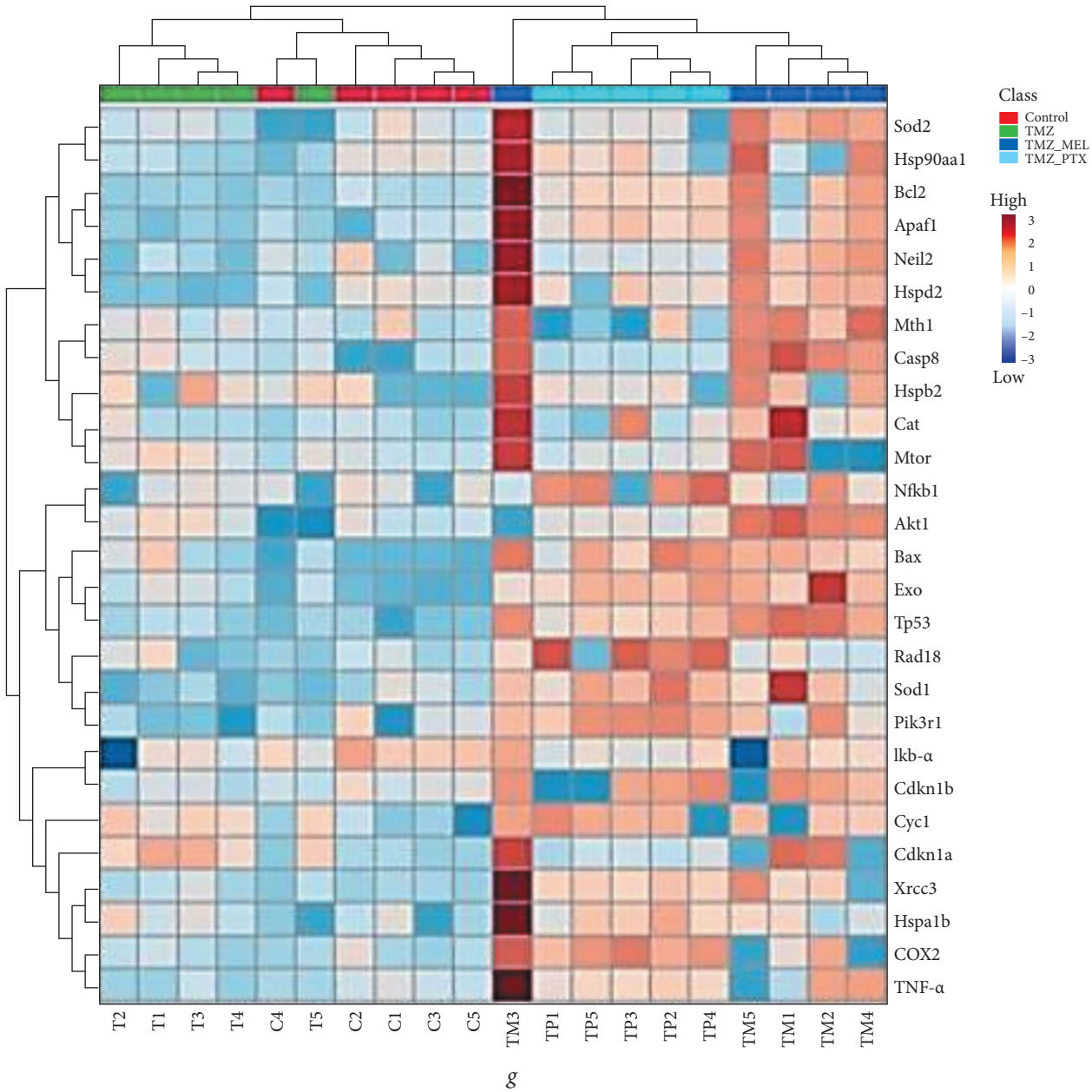

g

Fig. 4. Heat map analysis using gene expressions of C6 (*a*—*d*) and N1E-115 (*e*—*g*) cells for control, 1/2 IC_{50} chemotherapy dose of TMZ, and combinations with MEL and PTX treatment for 72 h. *a* and *e* — the resulting score plots; *b*, *c*, *f* — variable ımportance in projection (VIP) scores. All data are log (x + 1) transformed, and eBayes and Pearson correlation options were used for hierarchical clustering and correlation analysis, respectively

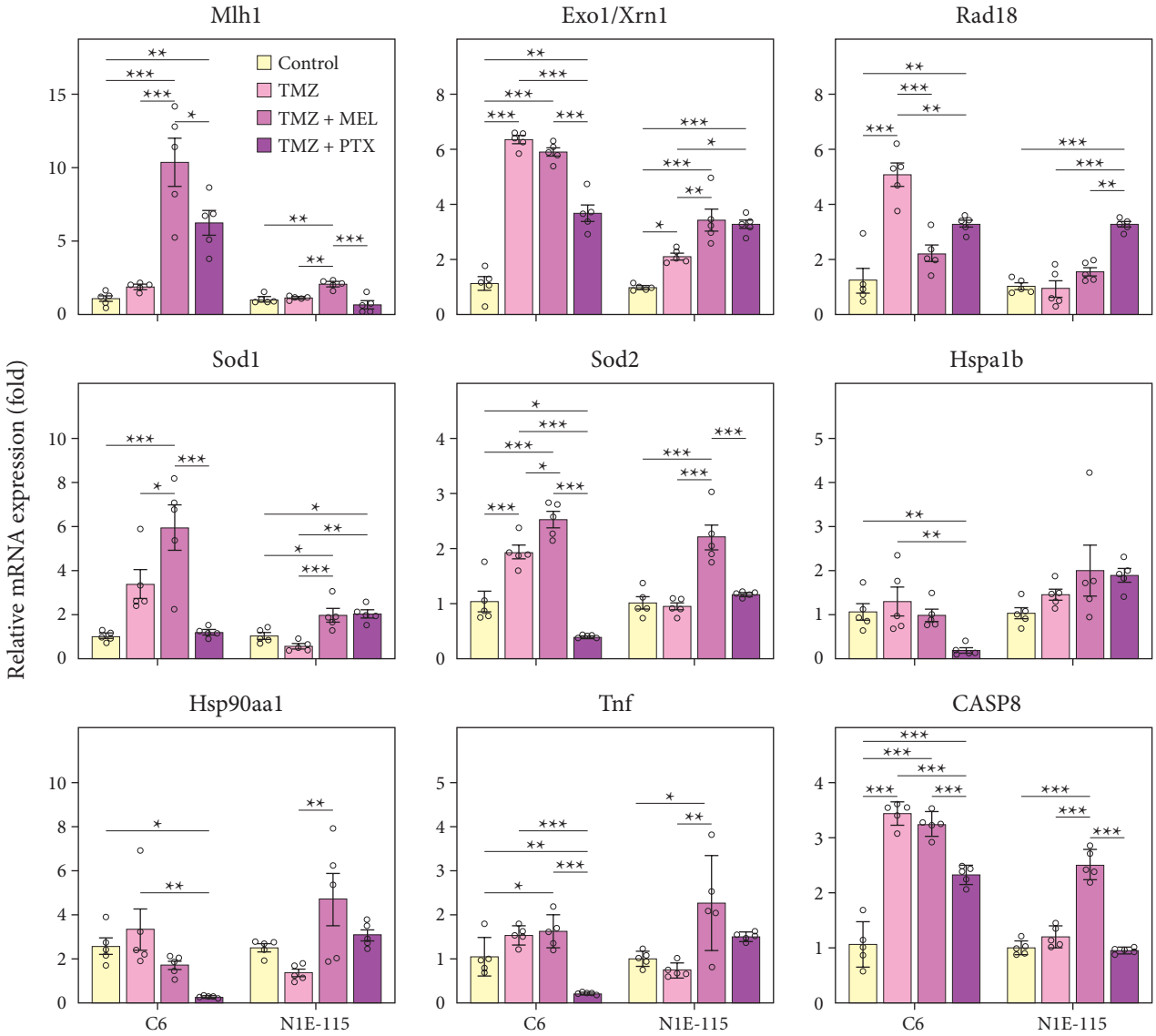

Fig. 5. Relative fold change determined by qRT-PCR analysis of the *Mlh1, Sod1, Exo1, Sod2, Rad18, Hspa1b,* and *Hsp90aa1* genes in C6 and N1E-115 cells. All data were normalized to *β-actin* expression and are given as relative to control (control = 1 not shown in the Figure). Data are presented as mean ± SE, n = 5, Mann — Whitney U test: $^{*}p \le 0.05$, $^{**}p \le 0.01$, $^{***}p \le 0.001$. Control — vehicle-treated cells

fewer side effects on healthy cells compared to the typical doses of TMZ alone or with PTX. Mechanistically, the combination treatment induces apoptotic pathways in cancer cells, contrasting with PTX-induced necrosis.

Studying human GBM U87-MG and MU1454 cell lines, McConnell et al. [29] discovered that the treatment with TMZ alone led to a 40% decrease in cell proliferation. However, combining 100 μM TMZ with 1 mM MEL resulted in a more significant reduction, with cell proliferation lowering by 60% compared to the control group. This outcome is linked to MEL capacity to elevate intracellular ROS levels and trigger oxidative stress in hypoxic cancer cells, notably those prevalent in brain tumors like glioblastoma [30, 31]. Research has indicated that the application of MEL is linked to an elevated production of ROS, primarily within mitochondria. This outcome was linked to different respiratory mechanisms, with a notable increase observed in the hypoxic conditions within cancerous cells [32, 33].

Genomic analyses further elucidated the upregulated expression of DNA repair genes (e.g. *Mlh1, Exo1, Xrcc3*, and *Neil2*) in response to TMZ + MEL treatment, indicating robust DNA damage responses in cancer cells. Additionally, MEL augmented heat shock responses and mitochondrial Hsp60

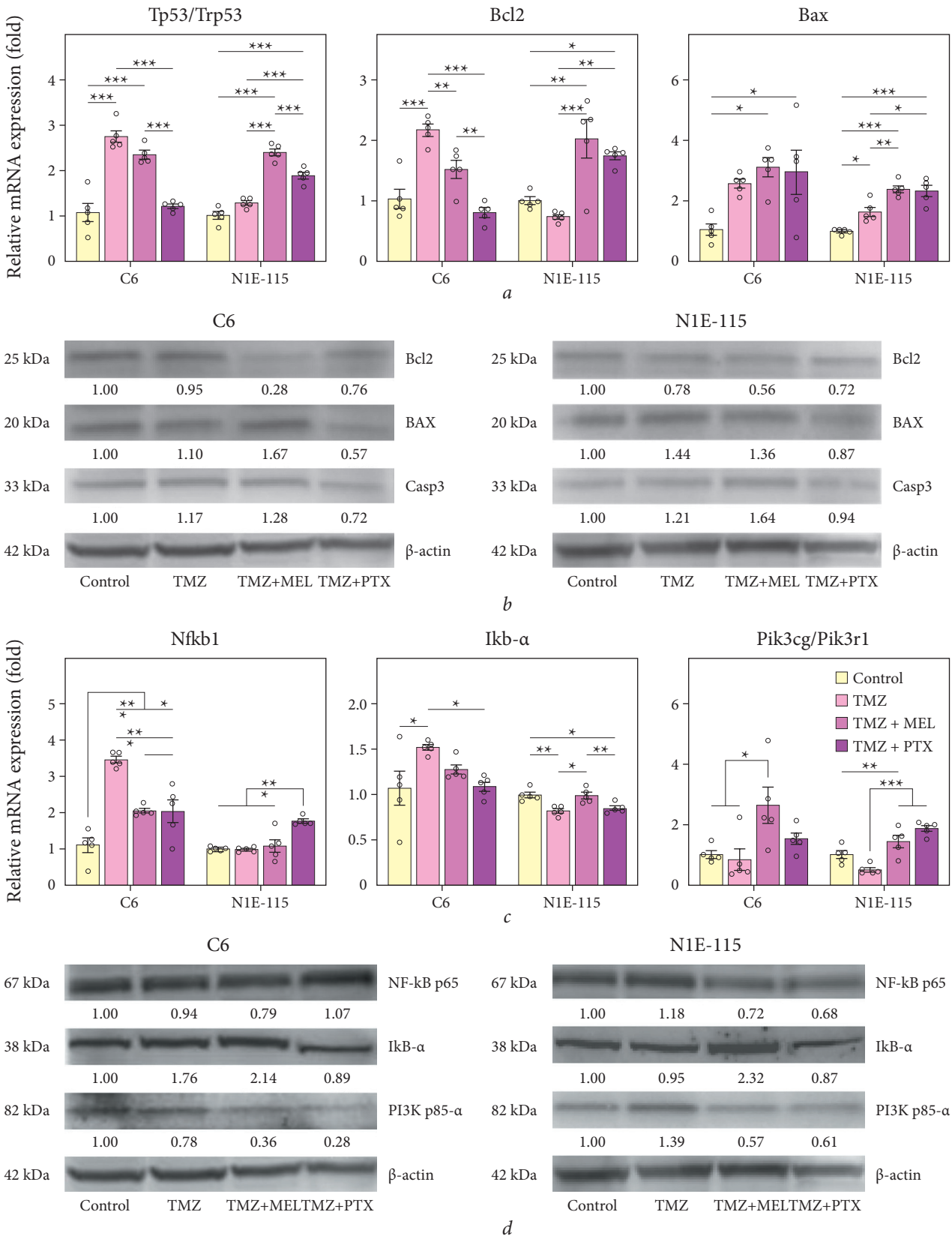

Fig. 6. Relative fold change determined by qRT-PCR analysis of *p53, Bcl2*, and *Bax* genes (*a*) and *Nfkb1, IkB-α,* and *Pik3cg* genes (*c*) in C6 and N1E-115 cells. All data were normalized to β-actin expression and are given relative to control. Data were presented as the mean ± SE, n = 5. * $p \le 0.05$; ** $p \le 0.01$; *** $p \le 0.001$. Control — vehicle-treated control. Western blot analysis with the relative intensity of Nfkb1, P53, Bcl2, and Bax proteins (*b*) and Nfkb1, IkB-α, and PI3K p8-α proteins (*d*) (relative intensity normalized to β-actin)

levels, while suppressing NF-κB signaling, thereby promoting apoptosis in glioblastoma cells and attenuating survival mechanisms.

The tumor suppressor protein p53 is a critical regulator of cellular stress responses, particularly in the induction of apoptosis [34]. Its activation leads to a series of events where *Bax* is upregulated, promoting the mitochondrial outer membrane permeabilization (MOMP) and the subsequent release of cytochrome c into the cytoplasm. This initiates the formation of the apoptosome and activation of caspase-3, culminating in apoptosis [35]. The findings revealed that TMZ and its combinations, especially with MEL, significantly increase p53 expression, thereby promoting apoptosis. This was evidenced by the increased expression of the downstream pro-apoptotic genes such as *Bax* and *Cycs* and elevated levels of caspase-3 protein, all of which are key components of the intrinsic apoptotic pathway. In C6 cells, the TMZ + MEL combination not only triggered the intrinsic pathway but also activated the extrinsic pathway, as indicated by the upregulation of *TNF-α* and *Casp8* gene expression. This dual activation suggests a robust apoptotic response, enhancing the therapeutic efficacy of the treatment. Furthermore, the synergistic effect observed with the TMZ and MEL combination indicates that MEL potentiates the p53-mediated apoptotic pathway, further supporting its role as an adjuvant in cancer therapy. Dramatically, in N1E-115 cells, while p53 expression increased in response to TMZ and its combinations, the activation of the mitochondrial apoptotic pathway was less pronounced compared to C6 cells. This suggests cell-type-specific differences in apoptotic signaling, where the extrinsic pathway might play a more dominant role in N1E-115 cells. The increased *Tp53* levels and associated cell cycle arrest in these cells imply that p53 also contributes to growth inhibition, adding another layer to its tumor suppressor function. The data aligns with the literature where TMZ-induced apoptosis in glioblastoma cells involves *Tp53* activation and subsequent mitochondrial dysfunction, cytochrome c release, and caspase activation [36, 37]. Moreover, the synergistic effects of MEL in enhancing p53-mediated apoptosis corroborate the findings from studies on hepatocellular carcinoma and glioblastoma, where MEL increases p53 and Bax expression while decreasing *Bcl2* levels [38, 39]. In summary, p53 plays a pivotal role in mediating the apoptotic effects of TMZ and its combinations with MEL or PTX. The enhanced p53 expression and activity lead to significant apoptosis via both intrinsic and extrinsic pathways with cell line-specific variations. These findings underscore the therapeutic potential of targeting p53 and its downstream effectors to optimize cancer treatment strategies. It also highlights the therapeutic promise of MEL-based combinatorial therapies in GBM and NB, emphasizing their potential to increase treatment efficacy while reducing adverse effects on healthy tissues. Future investigations should explore the translational implications of these findings in clinical oncology practice, paving the way for optimized and personalized cancer treatment strategies.

In conclusion, the combination of TMZ and MEL demonstrates decreased harm to healthy cells while retaining strong anti-proliferative effects similar to the TMZ and PTX treatment. Moreover, the combination allowed a significant reduction in the effective dose of TMZ, suggesting a potential strategy to mitigate chemotherapy-related side effects. Further validation through human cell culture studies and GMB and NB animal models is required to substantiate these results and evaluate the clinical feasibility of this combinatorial therapy. Overall, our data provide a foundation for future research on the efficacy and safety of TMZ and MEL therapy for GMB and NB, potentially offering new avenues to improve treatment outcomes in these challenging cancers.

Acknowledgment

This study was funded by the Trakya University Scientific Research (TUBAP-2018/292).

REFERENCES

1. Tang Q, Ren L, Liu J, et al. Withaferin A triggers G2/M arrest and intrinsic apoptosis in glioblastoma cells via ATF4-ATF3-CHOP axis. *Cell Prolif*. 2020;53(1):e12706. https://doi.org/10.1111/cpr.12706
2. de Souza I, Monteiro L, Guedes C, et al. High levels of NRF2 sensitize temozolomide-resistant glioblastoma cells to ferroptosis via ABCC1/MRP1 upregulation. *Cell Death Dis*. 2022;13(7):591. https://doi.org/10.1038/s41419-022-05044-9

3. Erthal LC, Shi Y, Sweeney KJ, et al. Nanocomposite formulation for a sustained release of free drug and drug-loaded responsive nanoparticles: an approach for a local therapy of glioblastoma multiforme. *Sci Rep*. 2023;13(1):5094. https://doi.org/10.1038/s41598-023-32257-5
4. Szklener K, Rodzajewska A, Kurylo W, Mandziuk S. New therapeutic strategies based on molecularly targeted therapy in glioblastoma – a case report and review of the literature. *Curr Issues Pharmacy Med Sci*. 2022;35(4):206-211. https://doi.org/10.2478/cipms-2022-0036
5. Li Y, Wan Y, Yu N, Zhao Y, Li M. Galangin (GLN) promotes temozolomide-induced apoptosis in glioma cells. *Biol Bull*. 2022;49(6):580-587. https://doi.org/10.1134/S1062359022060085
6. Kong Y, Feng Z, Chen A, et al. The natural flavonoid galangin elicits apoptosis, pyroptosis, and autophagy in glioblastoma. *Front Oncol*. 2019;9:942. https://doi.org/10.3389/fonc.2019.00942
7. Izadi A, Sadeghi A, Jalili-Nik M, et al. Combination of alpha-lipoic acid and auraptene ınduces apoptosis and prevents proliferation of the human U-87 glioblastoma cells. *Revista Brasileira Farmacognosia*. 2023;33(6):1177-1186. https://doi.org/10.1007/s43450-023-00440-4
8. Cai Q, Li X, Xiong H, et al. Optical blood-brain-tumor barrier modulation expands therapeutic options for glioblastoma treatment. *Nat Commun*. 2023;14(1):4934. https://doi.org/10.1038/s41467-023-40579-1
9. Li W, Xu X. Advances in mitophagy and mitochondrial apoptosis pathway-related drugs in glioblastoma treatment. *Front Pharmacol*. 2023;14. https://doi.org/10.3389/fphar.2023.1211719
10. Feng L, Li S, Wang C, Yang J, editors. *Current Status and Future Perspective on Molecular Imaging and Treatment of Neuroblastoma. Semin Nucl Med*; 2023: Elsevier. https://doi.org/10.1053/j.semnuclmed.2022.12.004
11. Gundem G, Levine MF, Roberts SS, et al. Clonal evolution during metastatic spread in high-risk neuroblastoma. *Nat Genet*. 2023:1-12. https://doi.org/10.1038/s41588-023-01395-x
12. Mañas A, Aaltonen K, Andersson N, et al. Clinically relevant treatment of PDX models reveals patterns of neuroblastoma chemoresistance. *Sci Adv*. 2022;8(43):eabq4617. https://doi.org/ 10.1126/sciadv.abq4617
13. Thirant C, Peltier A, Durand S, et al. Reversible transitions between noradrenergic and mesenchymal tumor identities define cell plasticity in neuroblastoma. *Nat Commun*. 2023;14(1):2575. https://doi.org/10.1038/s41467-023-38239-5
14. Del Bufalo F, De Angelis B, Caruana I, et al. GD2-CART01 for relapsed or refractory high-risk neuroblastoma. *N Engl J Med*. 2023;388(14):1284-1295. https://doi.org/10.1056/NEJMoa2210859
15. Erdogan CS, Al Hassadi Y, Aru B, et al. Combinatorial effects of melatonin and paclitaxel differ depending on the treatment scheme in colorectal cancer in vitro. *Life Sci*. 2022;308:120927. https://doi.org/10.1016/j.lfs.2022.120927
16. Graham-Gurysh EG, Murthy AB, Moore KM, et al. Synergistic drug combinations for a precision medicine approach to interstitial glioblastoma therapy. *J Control Release*. 2020;323:282-292. https://doi.org/10.1016/j.jconrel.2020.04.028
17. Sonabend AM, Gould A, Amidei C, et al. Repeated blood–brain barrier opening with an implantable ultrasound device for delivery of albumin-bound paclitaxel in patients with recurrent glioblastoma: a phase 1 trial. *Lancet Oncol*. 2023;24(5):509-522. https://doi.org/10.1016/S1470-2045(23)00112-2
18. Lelak K, Vohra V, Neuman MI, et al. Pediatric melatonin ıngestions—United States, 2012–2021. *MMWR Morb Mortal Wkly Rep*. 2022;71(22):725-729. https://doi.org/10.15585/mmwr.mm7122a1
19. Minocha T, Das M, Rai V, et al. Melatonin induces apoptosis and cell cycle arrest in cervical cancer cells via inhibition of NF-κB pathway. *Inflammopharmacology*. 2022;30(4):1411-1429. https://doi.org/10.1007/s10787-022-00964-6
20. Mafi A, Rezaee M, Hedayati N, et al. Melatonin and 5-fluorouracil combination chemotherapy: opportunities and efficacy in cancer therapy. *Cell Commun Signaling*. 2023;21(1):33. https://doi.org/10.1186/s12964-023-01047-x
21. Talib WH. A ketogenic diet combined with melatonin overcomes cisplatin and vincristine drug resistance in breast carcinoma syngraft. *Nutrition*. 2020;72:110659. https://doi.org/10.1016/j.nut.2019.110659
22. Chen K, Zhu P, Chen W, et al. Melatonin inhibits proliferation, migration, and invasion by inducing ROS-mediated apoptosis via suppression of the PI3K/Akt/mTOR signaling pathway in gallbladder cancer cells. *Aging (Albany NY)*. 2021;13(18):22502. https://doi.org/10.18632/aging.203561
23. Moloudizargari M, Moradkhani F, Hekmatirad S, et al. Therapeutic targets of cancer drugs: Modulation by melatonin. *Life Sci*. 2021;267:118934. https://doi.org/10.1016/j.lfs.2020.118934
24. Hernández-Cerón M, Chavarria V, Ríos C, et al. Melatonin in combination with albendazole or albendazole sulfoxide produces a synergistic cytotoxicity against malignant glioma cells through autophagy and apoptosis. *Brain Sci*. 2023;13(6):869. https://doi.org/10.3390/brainsci13060869
25. Ismail M, Yang W, Li Y, et al. Targeted liposomes for combined delivery of artesunate and temozolomide to resistant glioblastoma. *Biomaterials*. 2022;287:121608. https://doi.org/10.1016/j.biomaterials.2022.121608
26. Hamed AR, Yahya SM, Nabih HK. Anti-drug resistance, anti-inflammation, and anti-proliferation activities mediated by melatonin in doxorubicin-resistant hepatocellular carcinoma: In vitro investigations. *Naunyn-Schmiedeberg's Arch Pharmacol*. 2023:1-12. https://doi.org/10.1007/s00210-023-02385-w
27. Westhoff M-A, Karpel-Massler G, Brühl O, et al. A critical evaluation of PI3K inhibition in Glioblastoma and Neuroblastoma therapy. *Molec Cell Ther*. 2014;2(1):1-10. http://www.molcelltherapies.com/content/2/1/32
28. Tan BL, Norhaizan ME. Curcumin combination chemotherapy: The implication and efficacy in cancer. *Molecules*. 2019;24(14):2527. https://doi.org/10.3390/molecules24142527

29. McConnell DD, McGreevy JW, Williams MN, Litofsky NS. Do anti-oxidants vitamin D3, melatonin, and alpha-lipoic acid have synergistic effects with temozolomide on cultured glioblastoma cells? *Medicines*. 2018;5(2):58. https://doi.org/10.3390/medicines5020058
30. Huang P, Feng L, Oldham EA, Keating MJ, Plunkett W. Superoxide dismutase as a target for the selective killing of cancer cells. *Nature*. 2000;407(6802):390-395. https://doi.org/10.1038/35030140
31. Zhou Y, Hileman EO, Plunkett W, Keating MJ, Huang P. Free radical stress in chronic lymphocytic leukemia cells and its role in cellular sensitivity to ROS-generating anticancer agents. *Blood*. 2003;101(10):4098-4104. https://doi.org/10.1182/blood-2002-08-2512
32. Proietti S, Cucina A, Minini M, Bizzarri M. Melatonin, mitochondria, and the cancer cell. *Cell Molec Life Sci*. 2017;74:4015-4025. https://doi.org/10.1007/s00018-017-2612-z
33. Li M, Wu C, Muhammad JS, et al. Melatonin sensitises shikonin-induced cancer cell death mediated by oxidative stress via inhibition of the SIRT3/SOD2-AKT pathway. *Redox Biol*. 2020;36:101632. https://doi.org/10.1016/j.redox.2020.101632
34. Mantovani F, Collavin L, Del Sal G. Mutant p53 as a guardian of the cancer cell. *Cell Death Differ*. 2019;26(2):199-212. https://doi.org/10.1038/s41418-018-0246-9
35. Katiyar SK, Roy AM, Baliga MS. Silymarin induces apoptosis primarily through a p53-dependent pathway involving Bcl-2/Bax, cytochrome c release, and caspase activation. *Mol Cancer Ther*. 2005;4(2):207-216. https://doi.org/10.1158/1535-7163.207.4.2
36. Jakubowicz-Gil J, Langner E, Bądziul D, Wertel I, Rzeski WJTB. Apoptosis induction in human glioblastoma multiforme T98G cells upon temozolomide and quercetin treatment. *Tumor Biol*. 2013;34(4):2367-2378. https://doi.org/10.1007/s13277-013-0785-0
37. Günther W, Pawlak E, Damasceno R, et al. Temozolomide induces apoptosis and senescence in glioma cells cultured as multicellular spheroids. *Br J Cancer*. 2003;88(3):463-469.
38. Sánchez DI, González-Fernández B, Crespo I, et al. Melatonin modulates dysregulated circadian clocks in mice with diethylnitrosamine-induced hepatocellular carcinoma. *J Pineal Res*. 2018;65(3):e12506. https://doi.org/10.1111/jpi.12506
39. Zhou N, Wei ZX, Qi ZX. Inhibition of autophagy triggers melatonin-induced apoptosis in glioblastoma cells. *BMC Neurosci*. 2019;20(1):63. https://doi.org/10.1186/s12868-019-0545-1

Submitted: April 01, 2024

А. Бостанчі [1], О. Доганлар [2]
[1] Відділ генетики і біоінженерії, Тракійський університет, Едірне, Туреччина
[2] Відділ медичної біології, Тракійський університет, Едірне, Туреччина

МЕЛАТОНІН ПІДСИЛЮЄ АПОПТОЗ, ІНДУКОВАНИЙ ТЕМОЗОЛОМІДОМ, В КЛІТИНАХ ГЛІОБЛАСТОМИ І НЕЙРОБЛАСТОМИ

Стан питання. Сполучення темозоломіду (TMZ) та паклітакселу (PTX) зазвичай є найчастіше застосованим режимом хіміотерапії для лікування хворих на гліобластому. Однак приблизно у половини хворих розвивається стійкість до TMZ. До того ж, застосування цих засобів супроводжується серйозними побічними ефектами. Мелатонін (MEL), багатофункціональний гормон, може бути корисним у комбінованій протипухлинній терапії, оскільки він впливає на пухлинні клітини відмінно від нормальних клітин. **Мета** полягала в дослідженні *in vitro* інгібувального ефекту MEL у сполученні з TMZ на виживаність пухлинних клітин гліобластоми і нейробластоми. **Матеріали та методи**. У дослідженні використовували пухлинні клітини ліній C6 (*Rattus norvegicus*) та N1E-115 (*Mus musculus*), а також клітини C8-D1A нормальних астроцитів мишей. Проліферацію клітин оцінювали в MTT тесті. IC_{50} обраховували за допомогою пробіт-аналізу. Дві концентрації TMZ (IC_{50} та 1/2 IC_{50}) застосовували для індукції цитотоксичності в досліджуваних лініях клітин, а також досліджували вплив TMZ у сполученні з PXT або MEL. Аналіз індукції апоптозу проводили методом проточної цитометрії із застосуванням анексину та пропідію йодиду. Експресію генів, залучених до певних сигнальних шляхів, оцінювали кількісною полімеразною ланцюговою реакцією зі зворотною транскрипцією (qRT-PCR), а експресію відповідних білків визначали вестерн-блот аналізом. **Результати**. За даними MTT тесту TMZ у сполученні з MEL суттєво знижує життєздатність пухлинних клітин. За даними qRT-PCR таке сполучення приводить до підвищення експресії генів антиоксидантних ферментів (*Sod1, Sod2*) та генів репарації ДНК (*Mlh1, Exo1, Rad18*) в обох лініях пухлинних клітин. При цьому значно знижується рівень експресії *Nfkb1* та *Pik3cg*, збільшується затримка клітин за фазами циклу, підвищується експресія p53 та проапоптотичних білків (BAX та каспаза-3). **Висновки**. Сполучення MEL з низькою дозою TMZ може підвищувати індукцію апоптозу в пухлинних клітинах, що може в перспективі стати альтернативою застосування самого лише TMZ у лікуванні хворих на гліобластому.

Ключові слова: мелатонін, гліобластома, нейробластома, темозоломід.